Two-body nonleptonic decays of charmed mesons

P. Bedaque, A. Das, and V. S. Mathur
Department of Physics and Astronomy, University of Rochester, Rochester, New York 14627
(Received 16 July 1993)

Two-body nonleptonic decays of charmed mesons are studied on the basis of a simple pole-dominance model involving the vector, pseudoscalar, and axial-vector meson poles.

PACS number(s): 13.25.Ft, 12.40.Vv, 14.40.Lb

I. INTRODUCTION

In this paper, we calculate the two-body nonleptonic decays of charmed mesons using the pole-dominance model. A preliminary analysis of this type was first attempted [1] several years ago, but we believe that a systematic investigation of the type presented here has not been carried out. The nonleptonic weak decay of a pseudoscalar meson into two pseudoscalar mesons is parity violating, so in such decays the pole-dominance model would involve only vector-meson poles. It is well known [2] that this idea of vector dominance provides a successful description of the $K \rightarrow \pi\pi$ decays. Recently we have also discussed [3] the decay of D mesons into two pseudoscalars (PP) through vector dominance and there, too, we find reasonable agreement with experiments. In the present work we extend the analysis to the general two-body nonleptonic decays of D mesons to include the decay to a pseudoscalar and a vector (PV) meson and to two vector (VV) mesons. Since we now deal with parity-conserving decays as well, we have to go beyond vector dominance. In this work, we extend our consideration to include also the pseudoscalar and the axial-vector-meson poles. For simplicity, we consider only the lowest lying poles [4].

Our work has no direct relationship to the extensively studied factorization model [5] which has generally been quite successful in describing the decays except for those that proceed only through what are known as the annihilation diagrams. The pole-dominance model, on the other hand, has enjoyed many successes in low-energy hadron phenomenology, and it would be interesting to see how it describes charm decay [6].

II. PRELIMINARIES

For nonleptonic decay of charm, the effective weak Hamiltonian may be written in the current-current form as [7]

$$H_W = \frac{G_F}{\sqrt{2}}[a_1(\bar{u}d')_\mu(\bar{s}'c)_\mu + a_2(\bar{s}'d')_\mu(\bar{u}c)_\mu] , \quad (1)$$

where $(\bar{q}^\alpha q_\beta)_\mu$ are color-singlet $V-A$ currents

$$(\bar{q}^\alpha q_\beta)_\mu = i\bar{q}^\alpha\gamma_\mu(1+\gamma_5)q_\beta = (V_\mu)^\alpha_\beta + (A_\mu)^\alpha_\beta . \quad (2)$$

The indices $\alpha,\beta = 1,2,3,4$ represent the flavor SU(4) indices and a_1, a_2 are real coefficients which we treat as phenomenological parameters. The primed quark fields are related to the unprimed ones by the usual Cabibbo-Kobayashi-Maskawa (CKM) mixing matrix. For the nonleptonic decays of D mesons into two mesons, the Hamiltonian (1) leads to two main classes of quark-model diagrams, the spectator and the annihilation diagrams shown in Figs. 1(a) and 1(b), respectively. We ignore the Penguin-type contributions. It is well known that the annihilation-diagram contribution in the quark model is helicity suppressed.

In the pole-dominance model, we take the currents in H_W to be the hadronic currents given by the field current identities ($\alpha,\beta = 1,2,\ldots,4$)

$$(V_\mu)^\alpha_\beta = \sqrt{2}g_V(\phi_\mu)^\alpha_\beta ,$$
$$(A_\mu)^\alpha_\beta = \sqrt{2}f_P\partial_\mu P^\alpha_\beta + \sqrt{2}g_A(a_\mu)^\alpha_\beta , \quad (3)$$

where $(\phi_\mu)^\alpha_\beta$, P^α_β, and $(a_\mu)^\alpha_\beta$ are the field operators of the vector, the pseudoscalar and the axial-vector mesons of SU(4), respectively, and g_V, f_P, and g_A are the corresponding decay constants. The nonleptonic weak interaction can then be represented by a two-meson vertex which can be read off from (1) upon substituting (3).

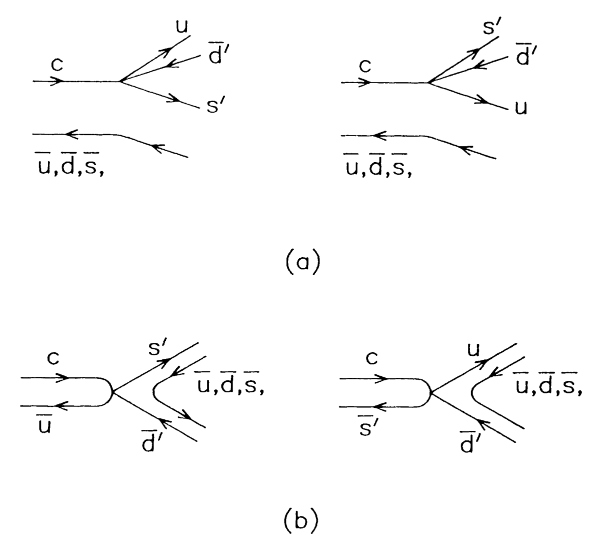

FIG. 1. Quark-model diagrams for the nonleptonic decay of D into two mesons. 1(a) describe the spectator diagrams and 1(b) the annihilation diagrams.

III. CALCULATION OF THE DECAY AMPLITUDE

The Feynman diagrams for the two-body decays $D \to PP$, PV, and VV are displayed in Figs. 2–4. In these figures, the dark dot represents a weak interaction vertex and the open circle a strong vertex. Also the dotted lines, solid lines, and wavy lines represent pseudoscalar, vector, and axial-vector mesons respectively. Note that the figures 2(b), 3(c), 3(e), 4(b), and 4(c) are the analogues of the annihilation diagrams in the quark model, the remaining figures corresponding to the spectator diagrams. Only the vector-meson pole contributes to the parity-violating decay $D \to PP$ as shown in Fig. 2. Also, since $D \to PV$ is a parity conserving decay, a diagram such as Fig. 3(b) where the pseudoscalar pole is replaced by a vector pole cannot contribute.

We have several types of strong vertices appearing in the diagrams. These include the VPP, VVP, VVV, and the VPA vertices. Unfortunately, many of these couplings are not known. For numerical work, we choose to relate these couplings by a suitable flavor symmetry. In fact the VVP and VVV couplings can be related to the VPP couplings through an extended spin-SU(4) symmetry. Accordingly, we take the strong Hamiltonian as

$$H_{\rm str} = ig \,{\rm Tr}\left[\phi_\mu P \overleftrightarrow{\partial}_\mu P - \frac{2}{M} \varepsilon_{\mu\nu\lambda\rho} P \partial_\mu \phi_\nu \partial_\lambda \phi_\rho + \frac{2}{3} F_{\mu\nu} \phi_\mu \phi_\nu - \frac{2}{9M^2} F_{\mu\nu} F_{\nu\lambda} F_{\lambda\mu} \right] . \quad (4)$$

This is an obvious generalization of the Sakita-Wali interaction Hamiltonian [8] which is relevant to flavor SU(3). In (4), the trace is over the SU(4) multiplets, g is the coupling constant and M represents a mass scale. We shall identify M with the mass of the decaying particle, and take g to be the $\rho\pi\pi$ coupling determined from the ρ width. The VPA interaction is not contained in (4) and will be taken to be [9]

$$H_{\rm str}(VPA) = i g_s M \,{\rm Tr}\{ \phi_\mu [P, a_\mu] \} + \frac{i g_d}{M} {\rm Tr}\{ \partial_\mu \phi_\nu [P, \partial_\nu a_\mu] \} . \quad (5)$$

Despite some attempts in the past [9,10], the coupling constants g_s and g_d have not been determined successfully. In our present analysis, we will treat these as unknown parameters.

It should be mentioned that experience based on flavor SU(3) symmetry indicates that coupling constants are better described by group symmetry than the masses. Furthermore, the vector-meson couplings may be expected to have a somewhat special status embodied through universality. At the present time, however, we can only hope that couplings related by the larger SU(4) symmetry are not unreasonable. Future experiments involving the strong decays of charmed vector or axial vector mesons would shed light on this issue.

The weak vertices in Figs. 2–4 involve the decay constants g_V, f_P, and g_A for various particles. Once again only a few of these are known from experiments. Now, spectral function sum rules [11,12] based on asymptotic flavor symmetries have been quite successful in the past, and we may use them here to obtain suitable relations. From asymptotic SU(4) symmetry, it is easy to derive [13] the result that g_V/m_V would be the same for all vector

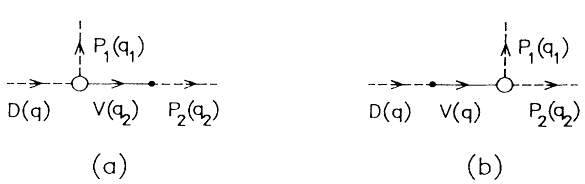

FIG. 2. Feynman diagrams for the decay $D \to P_1 P_2$.

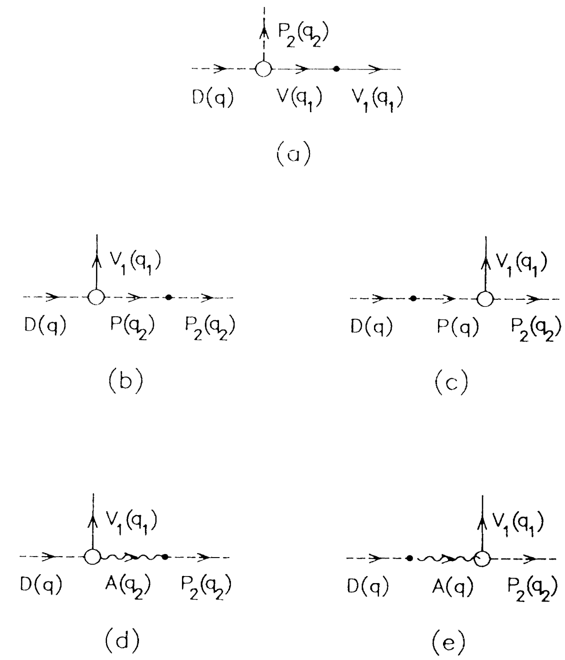

FIG. 3. Feynman diagrams for the decay $D \to V_1 P_2$.

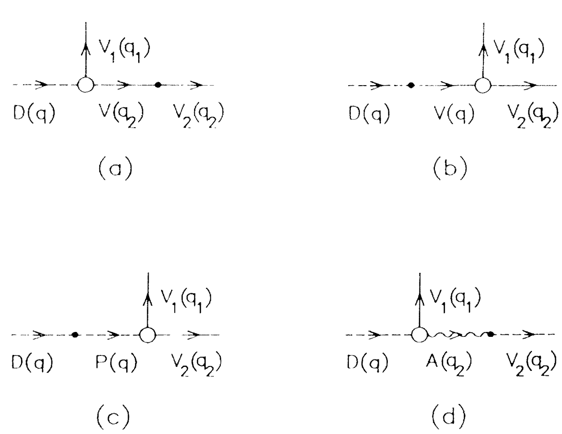

FIG. 4. Feynman diagrams for the decay $D \to V_1 V_2$.

TABLE I. Numerical values of the coupling constants and other parameters used in the paper.

Quantity	Value
g	4.28
g_V/m_V	152 MeV
f_π	92.6 MeV
f_K	1.2 f_π
f_η	f_π
$f_{\eta'}$	f_π
f_D	1.46 f_π
f_{D_S}	f_D
g_{A_1}/m_{A_1}	121 MeV
g_{K_1}/m_{K_1}	104 MeV
g_{f_1}/m_{f_1}	121 MeV
g_{D_1}/m_{D_1}	69.5 MeV
$g_{D_{S1}}/m_{D_{S1}}$	69.5 MeV

TABLE II. Amplitude A defined in Eq. (7) for the decay $D \to P_1 P_2$.

Decay	Amplitude A (10^6 GeV^{-1})
$D^0 \to K^- \pi^+$	$1.45(a_1 - 0.24 a_2)$
$D^0 \to \bar{K}^0 \pi^0$	$1.63 a_2$
$D^0 \to \bar{K}^0 \eta$	$0.50 a_2$
$D^+ \to \bar{K}^0 \pi^+$	$1.45(a_1 + 1.35 a_2)$
$D_S^+ \to \bar{K}^0 K^+$	$2.05 a_2$
$D_S^+ \to \eta \pi^+$	$-0.99 a_1$
$D_S^+ \to \eta' \pi^+$	$1.75 a_1$
$D^0 \to K^+ K^-$	$-0.39 a_1$
$D^0 \to K^0 \bar{K}^0$	0
$D^0 \to \pi^+ \pi^-$	$-0.37 a_1$
$D^0 \to \pi^0 \pi^0$	$-0.37 a_2$
$D^+ \to K^+ \bar{K}^0$	$-0.39 a_1$
$D^+ \to \pi^+ \pi^0$	$-0.26(a_1 + a_2)$
$D^+ \to \eta \pi^+$	$0.17 a_2 + 0.21 a_1$
$D^+ \to \eta' \pi^+$	$0.08 a_2 + 0.36 a_1$
$D_S^+ \to K^0 \pi^+$	$0.47 a_1$

mesons. Since we can extract g_ρ from the data on the decay $\rho \to l\bar{l}$, this result leads to a determination of all g_V. Also from asymptotic chiral SU(4) symmetry, we can derive the spectral function sum rule [14]

$$g_A^2/m_A^2 + f_P^2 = g_V^2/m_V^2 \ , \tag{6}$$

where A, P, and V are particles with the same internal quantum numbers. Now experimentally, only f_π and f_K are known. However, f_D has been determined [15] from QCD sum rules [16]. With the g_V's and f_P's known, the sum rule (6) then serves to determine the g_A's.

The numerical values of the various couplings used in our analysis are displayed in Table I. For the axial-vector-meson multiplet, we have taken the particles to be [17] $A_1(1260)$, $K_1(1400)$, $f_1(1285)$, $D_1(2420)$, and $D_{S_1}(2536)$.

The decay amplitudes for the PP, VP, and VV modes are defined as

$$M(D(q) \to P_1(q_1) P_2(q_2)) = \frac{-i(2\pi)^4 \delta^{(4)}(q - q_1 - q_2)}{\sqrt{2q_0 V 2q_{10} V 2q_{20} V}} iA \ , \tag{7}$$

$$M(D(q) \to V_1(q_1, \lambda_1) P_2(q_2)) = \frac{-i(2\pi)^4 \delta^{(4)}(q - q_1 - q_2)}{\sqrt{2q_0 V 2q_{10} V 2q_{20} V}} q_2 \cdot \varepsilon^{(\lambda_1)}(q_1) B \ , \tag{8}$$

$$M(D(q) \to V_1(q_1, \lambda_1) V_2(q_2, \lambda_2)) = \frac{-i(2\pi)^4 \delta^{(4)}(q - q_1 - q_2)}{\sqrt{2q_0 V 2q_{10} V 2q_{20} V}} [iC\delta_{\alpha\beta} + iD\varepsilon_{\mu\alpha\nu\beta} q_{1\mu} q_{2\nu} + iEq_{1\beta} q_{2\alpha}] \varepsilon_\alpha^{(\lambda_1)}(q_1) \varepsilon_\beta^{(\lambda_2)}(q_2) \ , \tag{9}$$

where $A, B, \ldots, E$ are constants representing the invariant amplitudes. The decay widths are easily calculated in terms of these amplitudes to be

$$\Gamma(D \to P_1 P_2) = \frac{1}{8\pi} \frac{k}{M^2} |A|^2 \ , \tag{10}$$

$$\Gamma(D \to V_1 P_2) = \frac{1}{8\pi} \frac{k^3}{m_1^2} |B|^2 \ , \tag{11}$$

$$\Gamma(D \to V_1 V_2) = \frac{1}{8\pi} \frac{k}{M^2} \left[|C|^2 \left\{ 3 + \frac{M^2 k^2}{m_1^2 m_2^2} \right\} - (CE^* + C^* E) \frac{M^2 (M^2 - m_1^2 - m_2^2)}{2 m_1^2 m_2^2} k^2 + |D|^2 2 M^2 k^2 + |E|^2 \frac{M^4 k^4}{m_1^2 m_2^2} \right] \ , \tag{12}$$

TABLE III. Amplitude B defined in Eq. (8) for the decay $D\to V_1P_2$.

Decay	Amplitude B (10^6)
$D^0\to K^{*-}\pi^+$	$2.16a_2+0.008a_1+0.323a_2(g_s-0.611g_d)-0.074a_1(g_s+0.382g_d)$
$D^0\to \bar{K}^{*0}\pi^0$	$-0.320a_2-0.230a_2(g_s-0.611g_d)$
$D^0\to \rho^+K^-$	$-2.16a_2+1.30a_1-0.323a_2(g_s-0.548g_d)$
$D^0\to \rho^0\bar{K}^0$	$1.64a_2+0.230a_2(g_s-0.548g_d)-0.066a_2(g_s+0.379g_d)$
$D^0\to \phi\bar{K}^0$	$2.16a_2+0.323a_2(g_s-0.614g_d)$
$D^0\to \omega\bar{K}^0$	$-1.43a_2-0.230a_2(g_s-0.554g_d)-0.066a_2(g_s+0.376g_d)$
$D^0\to \bar{K}^{*0}\eta$	$3.67a_2+0.388a_2(g_s-0.571g_d)$
$D^+\to \bar{K}^{*0}\pi^+$	$1.72a_2+0.008a_1-0.074a_1(g_s+0.382g_d)$
$D^+\to \rho^+\bar{K}^0$	$0.153a_2+1.30a_1-0.093a_2(g_s+0.379g_d)$
$D_S^+\to \rho^+\pi^0$	$-2.38a_1-0.565a_1(g_s-0.573g_d)$
$D_S^+\to K^{*+}\bar{K}^0$	$1.69a_1+0.153a_2+0.400a_1(g_s-0.570g_d)-0.098a_2(g_s+0.366g_d)$
$D_S^+\to \bar{K}^{*0}K^+$	$-1.56a_1+1.53a_2-0.400a_1(g_s-0.570g_d)$
$D_S^+\to \phi\pi^+$	$0.008a_1-0.078a_1(g_s+0.364g_d)$
$D_S^+\to \omega\pi^+$	0
$D_S^+\to \rho^+\eta$	$-0.756a_1$
$D_S^+\to \rho^+\eta'$	$1.68a_1$
$D^0\to K^{*-}K^+$	$0.355a_2+0.031a_1+0.085a_2(g_s-0.580g_d)-0.020a_1(g_s+0.350g_d)$
$D^0\to K^{*+}K^-$	$-0.355a_2+0.361a_1-0.085a_2(g_s-0.580g_d)$
$D^0\to \bar{K}^{*0}K^0$	$-0.029a_2-0.001a_2(g_s-0.580g_d)$
$D^0\to K^{*0}\bar{K}^0$	$0.029a_2+0.001a_2(g_s-0.580g_d)$
$D^+\to \bar{K}^{*0}K^+$	$-0.353a_1-0.086a_1(g_s-0.580g_d)-0.020a_1(g_s+0.350g_d)$
$D^+\to \phi\pi^+$	$0.479a_2$
$D^+\to \omega\pi^+$	$0.001a_1+0.228a_2-0.012a_1(g_s+0.409g_d)$
$D^+\to \rho^0\pi^+$	$0.541a_1-0.223a_2+0.122a_1(g_s-0.582g_d)+0.012a_1(g_s+0.413g_d)$
$D^+\to \rho^+\eta$	$-0.010a_2+0.196a_1+0.005a_2(g_s+0.373g_d)$
$D^+\to \rho^+\eta'$	$0.087_2+0.334a_1-0.011a_2(g_s+0.284g_d)$

where

$$k=\frac{1}{2M}[(M^2-m_1^2-m_2^2)^2-4m_1^2m_2^2]^{1/2}\ , \qquad (13)$$

M is the mass of the decaying particle and m_1, m_2 are the masses of the particles in the decay product. The amplitudes $A,B,\ldots,E$ can be written down from the Feynman diagrams in Figs. 2–4. Using the numerical values of the couplings in Table I, these can be expressed in terms of the four parameters: a_1, a_2, g_s, and g_d. The results for the Cabibbo allowed and once-suppressed decays are listed [18] in Tables II–IV.

IV. RESULTS

The decay amplitudes for $D\to PP$ listed in Table II, do not involve the parameters g_s and g_d. Thus it is best to obtain a fit for a_1 and a_2 from these decays. For this purpose we shall use the data on $D\to K\pi$ decays.

So far we have ignored the final state interactions. We shall take these into account by considering only elastic scattering in the final state. In $D\to K\pi$ decays, we have, in terms of isospin amplitudes,

TABLE IV. Amplitudes C, D, and E defined in Eq. (9) for the decay $D\to V_1V_2$.

Decay	Amplitudes		
	C $(10^6\ \text{GeV}^{-1})$	D $(10^6\ \text{GeV})$	E $(10^6\ \text{GeV})$
$D^0\to K^{*-}\rho^+$	$-0.215a_2-0.103a_1g_s$	$-1.16a_2-0.696a_1$	$0.030a_1g_d$
$D^0\to \bar{K}^{*0}\rho^0$	$0.152a_2-0.093a_2g_s$	$0.171a_2$	$0.027a_2g_d$
$D^0\to \bar{K}^{*0}\omega$	$-0.136a_2-0.093a_2g_s$	$-1.47a_2$	$0.027a_2g_d$
$D^+\to \bar{K}^{*0}\rho^+$	$-0.103a_1g_s-0.131a_2g_s$	$-0.924a_2-0.696a_1$	$0.030a_1g_d+0.038a_2g_d$
$D_S^+\to \phi\rho^+$	$-0.108a_1g_s$	$-0.660a_1$	$0.028a_1g_d$
$D_S^+\to K^{*+}\bar{K}^{*0}$	$-0.139a_2g_s$	$-0.873a_2-0.853a_1$	$0.036a_2g_d$
$D^0\to K^{*0}\bar{K}^{*0}$	0	$-0.241a_2$	0
$D^0\to \phi\rho^0$	$-0.025a_2g_s$	$-0.181a_2$	$0.007a_2g_d$
$D^+\to K^{*+}\bar{K}^{*0}$	$-0.028a_1g_s$	$-0.400a_1$	$0.008a_1g_d$
$D^+\to \phi\rho^+$	$-0.036a_2g_s$	$-0.256a_2$	$0.010a_2g_d$

$$A(D^0 \to K^-\pi^+) = \frac{1}{\sqrt{3}} A_{3/2} + \left[\frac{2}{3}\right]^{1/2} A_{1/2} ,$$
$$A(D^0 \to \bar{K}^0\pi^0) = \left[\frac{2}{3}\right]^{1/2} A_{3/2} - \frac{1}{\sqrt{3}} A_{1/2} , \quad (14)$$
$$A(D^+ \to \bar{K}^0\pi^+) = \sqrt{3} A_{3/2} ,$$

where

$$A_I = |A_I| e^{i\delta_I}$$

is the amplitude in the isospin state I and δ_I is the phase shift in that channel. Using the data from the particle properties data booklet [19], it is easy to obtain

$$|A_{1/2}| = 2.94\times 10^{-6} \text{ GeV} ,$$
$$|A_{3/2}| = 7.37\times 10^{-7} \text{ GeV} , \quad (15)$$
$$\delta_{1/2} - \delta_{3/2} = 93.4^\circ .$$

Now, in our model, the isospin amplitudes can be constructed if we invert the relations in Eq. (14) and use our results for the $D\to K\pi$ amplitudes from Table II. This gives

$$|A_{1/2}| = 1.18\times 10^{-6}(a_1 - 1.04 a_2) \text{ GeV} ,$$
$$|A_{3/2}| = 8.37\times 10^{-7}(a_1 + 1.35 a_2) \text{ GeV} . \quad (16)$$

Using the values for these amplitudes given by (15), we obtain the solution [20]

$$a_1 = 1.79, \quad a_2 = -0.67 . \quad (17)$$

There is another solution where $|a_2/a_1| > 1$, which we discard, as discussed in Ref. [3]. We also note that the result (17) is not very far from the values of a_1 and a_2 obtained by Bauer *et al.* [5].

With a_1 and a_2 determined, we fit g_s and g_d from the data on the decay modes $D\to PV$ and $D\to VV$. We find that the best fit corresponds to the values

$$g_s = -10.14, \quad g_d = -9.85 . \quad (18)$$

The branching ratios for various decay modes determined by our values of the parameters in (17) and (18) are exhibited in Tables V–VII, together with the experimental data. In preparing these tables, we have used, wherever possible, phase shifts for elastic scattering in the final state as determined from the data. Considering the uncertainties in our choice of the coupling constants, it is remarkable that most of our results are in reasonable agreement with the data.

TABLE V. Branching ratio for the decay $D\to P_1P_2$.

Decay	Branching ratio Theory	Experiment [19]
$D^0\to K^-\pi^+$	3.6×10^{-2}	$(3.65\pm 0.21)\times 10^{-2}$
$D^0\to \bar{K}^0\pi^0$	2.1×10^{-2}	$(2.1\pm 0.5)\times 10^{-2}$
$D^0\to \bar{K}^0\eta$	6.4×10^{-4}	$<2.3\times 10^{-2}$
$D^+\to \bar{K}^0\pi^+$	2.6×10^{-2}	$(2.6\pm 0.4)\times 10^{-2}$
$D_S^+\to \bar{K}^0K^+$	1.1×10^{-2}	$(2.8\pm 0.7)\times 10^{-2}$
$D_S^+\to \eta\pi^+$	2.0×10^{-2}	$(1.5\pm 0.4)\times 10^{-2}$
$D_S^+\to \eta'\pi^+$	5.1×10^{-2}	$(3.7\pm 1.2)\times 10^{-2}$
$D^0\to K^+K^-$	2.4×10^{-3}	$(4.1\pm 0.4)\times 10^{-3}$
$D^0\to K^0\bar{K}^0$	5.0×10^{-4}	$(1.1\pm 0.4)\times 10^{-3}$
$D^0\to \pi^+\pi^-$	1.6×10^{-3}	$(1.63\pm 0.19)\times 10^{-3}$
$D^0\to \pi^0\pi^0$	3.9×10^{-5}	$<4.6\times 10^{-3}$
$D^+\to K^+\bar{K}^0$	7.3×10^{-3}	$(7.3\pm 1.8)\times 10^{-3}$
$D^+\to \pi^+\pi^0$	1.5×10^{-3}	$<5.3\times 10^{-3}$
$D^+\to \eta\pi^+$	1.1×10^{-3}	$(6.6\pm 2.2)\times 10^{-3}$
$D^+\to \eta'\pi^+$	4.4×10^{-3}	$<8\times 10^{-3}$
$D_S^+\to K^0\pi^+$	4.5×10^{-3}	$<6\times 10^{-3}$

TABLE VI. Branching ratio for the decay $D\to V_1P_2$.

Decay	Branching ratio Theory	Experiment [19]
$D^0\to K^{*-}\pi^+$	1.4×10^{-2}	$(4.5\pm 0.6)\times 10^{-2}$
$D^0\to \bar{K}^{*0}\pi^0$	6.8×10^{-3}	$(2.1\pm 1.0)\times 10^{-2}$
$D^0\to \rho^+K^-$	10.2×10^{-2}	$(7.3\pm 1.1)\times 10^{-2}$
$D^0\to \rho^0\bar{K}^0$	1.3×10^{-2}	$(6.1\pm 3.0)\times 10^{-3}$
$D^0\to \phi\bar{K}^0$	1.1×10^{-3}	$(8.8\pm 1.2)\times 10^{-3}$
$D^0\to \omega\bar{K}^0$	1.8×10^{-3}	$(2.5\pm 0.5)\times 10^{-2}$
$D^0\to \bar{K}^{*0}\eta$	1.0×10^{-2}	$(2.1\pm 1.2)\times 10^{-2}$
$D^+\to \bar{K}^{*0}\pi^+$	1.4×10^{-2}	$(1.9\pm 0.7)\times 10^{-2}$
$D^+\to \rho^+\bar{K}^0$	6.4×10^{-2}	$(6.6\pm 1.7)\times 10^{-2}$
$D_S^+\to \rho^+\pi^0$	2.2×10^{-3}	$<2.2\times 10^{-3}$
$D_S^+\to K^{*+}\bar{K}^0$	1.6×10^{-2}	$(3.3\pm 0.9)\times 10^{-2}$
$D_S^+\to \bar{K}^{*0}K^+$	3.6×10^{-3}	$(2.6\pm 0.5)\times 10^{-2}$
$D_S^+\to \phi\pi^+$	3.5×10^{-2}	$(2.8\pm 0.5)\times 10^{-2}$
$D_S^+\to \omega\pi^+$	0	$<1.4\times 10^{-2}$
$D_S^+\to \rho^+\eta$	3.3×10^{-2}	$(7.9\pm 2.1)\times 10^{-2}$
$D_S^+\to \rho^+\eta'$	4.4×10^{-2}	$(9.5\pm 2.7)\times 10^{-2}$
$D^0\to K^{*-}K^+$	2.2×10^{-3}	$(2.0\pm 1.0)\times 10^{-3}$
$D^0\to K^{*+}K^-$	2.9×10^{-3}	$(3.5\pm 0.8)\times 10^{-3}$
$D^0\to \bar{K}^{*0}K^0$	2.0×10^{-6}	$<1.6\times 10^{-3}$
$D^0\to K^{*0}\bar{K}^0$	2.0×10^{-6}	$<8\times 10^{-4}$
$D^+\to \bar{K}^{*0}K^+$	5.3×10^{-3}	$(4.7\pm 0.9)\times 10^{-3}$
$D^+\to \phi\pi^+$	1.7×10^{-3}	$(6.0\pm 0.8)\times 10^{-3}$
$D^+\to \omega\pi^+$	1.1×10^{-3}	$<6\times 10^{-3}$
$D^+\to \rho^0\pi^+$	1.1×10^{-3}	$<1.2\times 10^{-3}$
$D^+\to \rho^+\eta$	5.1×10^{-3}	$<1.0\times 10^{-2}$
$D^+\to \rho^+\eta'$	9.6×10^{-4}	$<1.4\times 10^{-2}$

TABLE VII. Branching ratio for the decay $D\to V_1V_2$.

Decay	Branching ratio Theory	Experiment [19]
$D^0\to K^{*-}\rho^+$	6.5×10^{-2}	$(6.2\pm 2.5)\times 10^{-2}$
$D^0\to \bar{K}^{*0}\rho^0$	8.5×10^{-3}	$(1.5\pm 0.6)\times 10^{-2}$
$D^0\to \bar{K}^{*0}\omega$	7.9×10^{-3}	$<1.5\times 10^{-2}$
$D^+\to \bar{K}^{*0}\rho^+$	4.3×10^{-2}	$(4.1^{+1.5}_{-1.2})\times 10^{-2}$
$D_S^+\to \phi\rho^+$	5.7×10^{-2}	$(5.2^{+1.4}_{-1.6})\times 10^{-2}$
$D_S^+\to K^{*+}\bar{K}^{*0}$	1.5×10^{-2}	$(5.0\pm 1.7)\times 10^{-2}$
$D^0\to K^{*0}\bar{K}^{*0}$	2.6×10^{-5}	$(2.7^{+1.5}_{-1.2})\times 10^{-3}$
$D^0\to \phi\rho^0$	2.2×10^{-4}	$(1.8\pm 0.5)\times 10^{-3}$
$D^+\to K^{*+}\bar{K}^{*0}$	5.9×10^{-3}	$(2.6\pm 1.1)\times 10^{-2}$
$D^+\to \phi\rho^+$	1.2×10^{-3}	$<1.3\times 10^{-2}$

It should be remarked that our parameter fit in (17) and (18) leads to a destructive interference between the pseudoscalar and axial-vector meson poles in the annihilation diagrams in $D \rightarrow PV$. Thus decays such as $D^0 \rightarrow \phi \bar{K}^0$ and $D_S^+ \rightarrow \rho^+ \pi^0$ which proceed only through the annihilation diagrams lead to tiny branching ratios due to large cancellations in the contributions of Figs. 3(c) and 3(e). Unfortunately, because of this, small changes in our choice of the couplings can get magnified in the prediction of these branching ratios [21]. We would also like to point out that in $D \rightarrow VV$ decays, we did not consider the diagram analogous to 4(c) where the pseudoscalar meson pole is replaced by an axial-vector meson. There is no straightforward way of estimating the AVV strong coupling. The general agreement of our results with experiments in fact shows that the axial-vector pole diagram in $D \rightarrow VV$ may be neglected. It also shows that the simple pole model considered in this paper generally works quite well.

ACKNOWLEDGMENTS

This work was covered in part by the U.S. Department of Energy Grant No. DE-FG-02-91ER40685.

[1] V. S. Mathur, in *Proceedings of a Conference on Quark Confinement and Field Theory,* Rochester, 1976, edited by D. R. Stump and D. H. Weingarten (Wiley, New York, 1976).

[2] J. J. Sakurai, Phys. Rev. **156**, 1508 (1967).

[3] Ashok Das and Vishnu S. Mathur, Mod. Phys. Lett. A **8**, 2079 (1993).

[4] The inclusion of higher lying poles will introduce a large number of unknown parameters, and thus destroy any hopes of an experimental confrontation of the model.

[5] M. Bauer, B. Stech, and M. Wirbel, Z. Phys. C **34**, 103 (1987).

[6] For a description of other methods used in the study of charm decay, see the review papers by M. Wirbel, Prog. Part. Nucl. Phys. **21**, 33 (1988); R. J. Morrison and M. S. Witherell, Annu. Rev. Nucl. Part. Sci. **39**, 183 (1989).

[7] K. Jagannathan and V. S. Mathur, Nucl. Phys. **B171**, 78 (1980); and Ref. [5].

[8] B. Sakita and K. C. Wali, Phys. Rev. Lett. **14**, 404 (1965); Phys. Rev. **139**, B1355 (1965); A. Salaam, R. Delbourgo, and J. Strathdee, Proc. R. Soc. London **284**, 146 (1965).

[9] T. Das, V. S. Mathur, and S. Okubo, Phys. Rev. Lett. **19**, 1067 (1967); H. J. Schnitzer and S. Weinberg, Phys. Rev. **164**, 1828 (1967).

[10] V. S. Mathur, Phys. Rev. **174**, 1743 (1968).

[11] S. Weinberg, Phys. Rev. Lett. **18**, 507 (1967).

[12] T. Das, V. S. Mathur, and S. Okubo, Phys. Rev. Lett. **18**, 761 (1967). In the present paper, we use only the pole-dominated form of the first spectral-function sum rule.

[13] T. Das, V. S. Mathur, and S. Okubo, Phys. Rev. Lett. **19**, 470 (1967).

[14] This is a generalization to chiral SU(4) of the original (pole-dominated) first spectral-function sum rule of Weinberg (Refs. [11] and [12]). Note, in passing, that (6) leads to the upper bound $f_P < g_V / m_V = 152$ MeV.

[15] We use the value determined by V. S. Mathur and M. T. Yamawaki, Phys. Rev. D **29**, 2057 (1984). See also S. Narison, Phys. Lett. B **198**, 104 (1987); C. A. Dominguez and N. Paver, *ibid.* **197**, 423 (1987).

[16] M. Shifman, A. Vainshtein, and V. Zakharov, Nucl. Phys. **B147**, 385 (1979); **B147**, 448 (1979).

[17] D. W. G. S. Leith, in *Proceedings of the 6th NATO Advanced Study Institute on Techniques and Concepts of High-Energy Physics VI,* edited by Thomas Ferbel (Plenum, New York, 1991).

[18] Only those decay modes have been listed for which there are some experimental data.

[19] Particle Data Group, K. Hikasa *et al.*, Phys. Rev. D **45**, S1 (1992). We have ignored the errors quoted in the data for our analysis here. A recent paper of the CLEO Collaboration has quoted the $D \rightarrow \pi\pi$ branching ratios as $B(D^0 \rightarrow \pi^+\pi^-) = (0.127 \pm 0.011 \pm 0.011)\%$, $B(D^0 \rightarrow \pi^0\pi^0) = (0.080 \pm 0.015 \pm 0.014)\%$, $B(D^+ \rightarrow \pi^+\pi^0) = (0.22 \pm 0.05 \pm 0.05)\%$. We thank E. H. Thorndike for bringing these results to our attention.

[20] These values of a_1 and a_2 are slightly different from those in Ref. [3] since we have used a slightly different value of the strong coupling constant g.

[21] In fact the fit (18) for g_s and g_d was fine-tuned to reproduce the experimental bound for the decay $D_S^+ \rightarrow \rho^+ \pi^0$.